doi:10.1093/brain/awx085 BRAIN 2017: 140; 1643–1656 | 1643

BRAIN
A JOURNAL OF NEUROLOGY

Inhibition of the P2X7–PANX1 complex suppresses spreading depolarization and neuroinflammation

Shih-Pin Chen,[1,2,3] Tao Qin,[1] Jessica L. Seidel,[1] Yi Zheng,[1] Matthias Eikermann,[4] Michel D. Ferrari,[5] Arn M. J. M. van den Maagdenberg,[5,6] Michael A. Moskowitz,[7] Cenk Ayata[1,8] and Katharina Eikermann-Haerter[1]

Spreading depolarization is a wave of neuronal and glial depolarization. Within minutes after spreading depolarization, the neuronal hemichannel pannexin 1 (PANX1) opens and forms a pore complex with the ligand-gated cation channel P2X7, allowing the release of excitatory neurotransmitters to sustain spreading depolarization and activate neuroinflammation. Here, we explore the hypothesis that the P2X7–PANX1 pore complex is a critical determinant of spreading depolarization susceptibility with important consequences for neuroinflammation and trigeminovascular activation. We found that genetic loss of function or ablation of the *P2x7* gene inhibits spreading depolarization. Moreover, pharmacological suppression of the P2X7–PANX1 pore complex inhibits spreading depolarization in mice carrying the human familial hemiplegic migraine type 1 R192Q missense mutation as well as in wild-type mice and rats. Pore inhibitors elevate the electrical threshold for spreading depolarization, and reduce spreading depolarization frequency and amplitude. Pore inhibitors also suppress downstream consequences of spreading depolarization such as upregulation of interleukin-1 beta, inducible nitric oxide synthase and cyclooxygenase-2 in the cortex after spreading depolarization. In addition, they inhibit surrogates for trigeminovascular activation, including expression of calcitonin gene-related peptide in the trigeminal ganglion and c-Fos in the trigeminal nucleus caudalis. Our results are consistent with the hypothesis that the P2X7–PANX1 pore complex is a critical determinant of spreading depolarization susceptibility and its downstream consequences, of potential relevance to its signature disorders such as migraine.

1 Neurovascular Research Lab, Department of Radiology, Massachusetts General Hospital, Harvard Medical School, Charlestown, MA, USA
2 Department of Neurology, Neurological Institute, Taipei Veterans General Hospital, Taipei, Taiwan
3 Institute of Clinical Medicine, National Yang-Ming University School of Medicine, Taipei, Taiwan
4 Department of Anesthesia, Critical Care, and Pain Medicine, Massachusetts General Hospital, Boston, MA and Universitaet Duisburg Essen, Essen, Germany
5 Department of Neurology, Leiden University Medical Centre, 2300 RC Leiden, The Netherlands
6 Department of Human Genetics, Leiden University Medical Centre, 2300 RC Leiden, The Netherlands
7 Stroke and Neurovascular Regulation Laboratory, Departments of Radiology and Neurology, Massachusetts General Hospital, Charlestown, MA, USA
8 Stroke Service and Neuroscience Intensive Care Unit, Department of Neurology, Massachusetts General Hospital, Harvard Medical School, Boston, MA, USA

Correspondence to: Dr Katharina Eikermann-Haerter,
Assistant Professor of Radiology, 149 13th Street, Charlestown, MA 02129, USA
E-mail: khaerter@mgh.harvard.edu

Keywords: neuroinflammation; migraine; purinergic receptor; spreading depression; trigeminovascular activation

Received April 9, 2016. Revised January 18, 2017. Accepted February 12, 2017. Advance Access publication April 20, 2017

Abbreviations: CGRP = calcitonin gene-related peptide; Cox-2 = cyclooxygenase 2; FHM1 = familial hemiplegic migraine type 1; IL-1β = interleukin-1 beta; iNOS = inducible nitric oxide synthase; $P2X7_{chann}$ = P2X7 ligand-gated cation channel; $P2X7/PANX1_{pore}$ = P2X7–PANX1 pore complex; SD = spreading depolarization

Introduction

Animal and human studies underscore the importance of spreading depolarization as the electrophysiological event underlying migraine aura, and as a trigger for neuroinflammatory cascades implicated in headache pathogenesis (Moskowitz *et al.*, 1993; Hadjikhani *et al.*, 2001; Somjen, 2001; Bolay *et al.*, 2002; Karatas *et al.*, 2013). Recent animal experiments suggest that spreading depolarization-induced opening of the neuronal hemichannel pannexin 1 (encoded by *PANX1*) participates in the initiation of neuroinflammatory events in the brain and meninges during a migraine attack (Karatas *et al.*, 2013). PANX1, which opens immediately after spreading depolarization (Karatas *et al.*, 2013), is believed to promote large pore formation by tightly coupling to the neuronal purinergic P2X7 receptor after its activation (Pelegrin and Surprenant, 2006; Iglesias *et al.*, 2008). The large pore, presumably the 'P2X7–PANX1 pore complex' ($P2X7/PANX1_{pore}$), forms after P2X7 activation, mediated by a Src tyrosine kinase (Iglesias *et al.*, 2008). The $P2X7/PANX1_{pore}$ is permeable to molecules up to 900 Da (Pelegrin and Surprenant, 2006; Iglesias *et al.*, 2008) and mediates non-exocytotic glutamate release (Cervetto *et al.*, 2013; Di Cesare Mannelli *et al.*, 2015), which is potentially relevant for spreading depolarization susceptibility. P2X7 might also play a role independent of PANX1 in determining spreading depolarization susceptibility as a 'ligand-gated cation channel' ($P2X7_{chann}$), which transports small cations such as K^+ and Ca^{2+}, and mediates exocytotic glutamate release (Cervetto *et al.*, 2012). The two conformation forms of the P2X7 receptor, i.e. the ion-channel form and pore form, can also be activated via independent pathways. The $P2X7/PANX1_{pore}$ can be activated through intracellular signalling pathways via the Src homology 3 death domain of the C-terminus of the P2X7 receptor (Iglesias *et al.*, 2008), and the Src kinase involved in pore opening can, for example, be activated by glutamate (Weilinger *et al.*, 2012). Calmidazolium has been used as a drug to dissociate functions of the rapid gated ion channel from the pore form of P2X7R, because it inhibits selectively the $P2X7_{chann}$ without affecting pore function (Virginio *et al.*, 1997; Chessell *et al.*, 1998; Pelegrin and Surprenant, 2009; Cervetto *et al.*, 2012).

Animal models of spreading depolarization including transgenic knock-in mice that carry human familial hemiplegic migraine type 1 (FHM1) gene missense mutations introduced in the *Cacna1a* gene (van den Maagdenberg *et al.*, 2004, 2010; Eikermann-Haerter *et al.*, 2009; Ferrari *et al.*, 2015) provide a valuable platform for screening drugs used in antimigraine therapy (Ayata *et al.*, 2006; Eikermann-Haerter *et al.*, 2012*a*). Here, we examined whether inhibition of the $P2X7/PANX1_{pore}$, and/or $P2X7_{chann}$ suppresses spreading depolarization, and inhibits the consequent expression of inflammatory markers in cortex, and in the trigeminovascular system. Our findings underscore the importance of P2X7 and the pore complex as a determinant of spreading depolarization susceptibility, and downstream consequences such as neuroinflammation and activation of the trigeminovascular system.

Material and methods

Ethics

All experimental procedures were carried out in accordance with the Guide for Care and Use of Laboratory Animals (NIH Publication No. 85-23, 1996), and were approved by the institutional review board (Subcommittee on Research Animal Care of Massachusetts General Hospital and Taipei Veterans General Hospital).

Animals

We used 162 adult male Sprague-Dawley rats, 12 Balb/c and 103 C57BL/6J mice (Charles River and Jackson Laboratories). In addition, we compared eight P2X7 knockout mice (KO; $P2rx7^{-/-}$; B6.129P2-$P2rx7^{tm1Gab}$/J, stock 005576; Jackson Laboratory) to wild-type controls (C57BL/6J), and investigated six homozygous $Cacna1a^{R192Q}$ knock-in mice that carry the human FHM1 R192Q missense mutation in the *Cacna1a* gene resulting in a gain-of-function of $Ca_V2.1$ channel function (mutant mice were backcrossed for more than 10 generations on C57BL/6) (van den Maagdenberg *et al.*, 2004). The sample size of animals was estimated based on previous studies on spreading depression susceptibility. Rats were housed in groups of two to three per cage and mice were housed in groups of three to four per cage in a temperature-controlled room (21°C, 40–70% humidity, 12-h light–dark) and were acclimatized in the animal facility for at least 4 days prior to use. Animals had food and water *ad libitum* and experiments were performed during the light phase of the cycle. All animals were sacrificed immediately after data acquisition.

Surgical procedure and electrophysiological recordings

Animals were anaesthetized with 1.5% isoflurane in 30% O_2/70% N_2O. Rats were intubated and mechanically

ventilated (SAR-830; CWE), and mice were breathing spontaneously. Femoral arterial catheterization was performed for blood pressure monitoring and blood gas sampling in all animals. Blood pressure was monitored continuously with an intra-arterial pressure transducer. Arterial blood was collected every 15–30 min for determination of pH, PaO_2, and $PaCO_2$ (Rapidlab 248 blood gas/pH analyzer, Siemens HealthCare). Rectal temperature was kept between 36.9 and 37.1°C using a thermostatically controlled heating pad (Harvard Apparatus). All physiological parameters were maintained within normal range (Supplementary Table 1). Animals were placed on a stereotactic frame (Stoelting), and craniotomies were drilled under saline cooling. Coordinates of cranial windows were chosen according to the purpose of drug treatment, spreading depression induction, and recording (Figs 1A, 1D, 2A, 3A and 4A). In rats, the dura overlying the cortex at the craniotomies was gently removed and care was taken to avoid bleeding. In mice, the dura was kept intact. The electrocorticogram and direct-current (DC) potential were recorded with glass capillary microelectrodes. Signals were amplified with a DC preamplifier (EX1 differential amplifiers, Dagan Corporation) and continuously recorded (PowerLab, ADInstruments).

Experimental design

Pharmacological agents (Supplementary Table 2) were administered to inhibit: (i) $P2X7_{chann}$ and $P2X7/PANX1_{pore}$ (Brilliant blue G and A438079); (ii) $P2X7_{chann}$ only (calmidazolium); (iii) $P2X7/PANX1_{pore}$ only (Brilliant blue FCF); and (iv) the coupling between P2X7 and PANX1 (Src tyrosine kinase inhibitor PP2). Dose, route and timing of administration of all drugs were adopted from previous studies (Akaike and Himori, 2002; Iglesias *et al.*, 2008; Cervetto *et al.*, 2012; Chu *et al.*, 2012; Wang *et al.*, 2013). In this study, we used four routes of drug administration: (i) topical treatment with drug-adsorbed cotton balls (in both rats and mice); (ii) intracerebroventricular injection (in rats only); (iii) large cranial window with drug bath (in mice only); and (iv) intraperitoneal injection (in mice only). For experiments adopting topical treatment, three small cranial windows created over the occipital cortex (stimulation site for cortical spreading depression induction; rats: AP −4.5 mm, ML 2 mm; mice: AP −3 mm, ML 1.5 mm), parietal (proximal recording site; rats: AP −1.5 mm, ML 2 mm; mice: AP −1.5 mm, ML 1.5 mm), and frontal area (distal recording site; rats: AP 1.5 mm, ML 2 mm; mice: AP 1 mm, ML 1 mm) were pretreated with drug-adsorbed cotton balls. In experiments using topical treatment, one hemisphere was treated with drug, and the other hemisphere was treated with vehicle; the sequences of treatment were randomized in consecutive animals. For experiments using intracerebroventricular injection, a burr hole was created at the left hemisphere with the following coordinates: AP: −0.92 mm, ML: −1.50 mm. We performed intracerebroventricular injection in rats because we could not ascertain the effective cortical concentration after topical application of dyes (Brilliant blue G and Brilliant blue FCF) considering meningeal thickness and CSF flow. For experiments using large cranial window with drug bath (only in mice), a cranial window with an inner diameter of 3 mm was created over the parieto-occipital cortex and the drug solution was secured by a plastic ring. The drug-bathed cranial window served as either the stimulating or recording site depending on the purpose of experiments. The single investigator conducting the *in vivo* studies (S.P.C.) was blinded to the treatment groups except in experiments using coloured dyes (Brilliant blue G and Brilliant blue FCF) when blinding was not possible. The blinding was performed by concealment of treatments with individually and uniquely coded vials, and the order of treatments was randomized by drawing vial code numbers.

Four paradigms to assess spreading depolarization susceptibility were adopted. Paradigm 1: continuous topical KCl application to measure spreading depolarization frequency (Figs 1, 5B and 6). A cotton ball soaked with drugs or vehicles and KCl (1 M for rats and 300 mM for mice) was placed on the occipital cortex. Amplitude shifts in extracellular DC potential >5 mV were considered as spreading depression events. Paradigm 2: to determine the electrical threshold for spreading depolarization induction (Fig. 2A), single-squared pulses of increasing duration and intensity were applied to the cortex every 4 min (1–2048 μC), using a stimulus isolator (WPI) and a bipolar stimulation electrode (400 μm tip diameter, 1 mm tip separation; Frederick Haer Company), as previously described (Eikermann-Haerter *et al.*, 2011). Paradigm 3: repetitive suprathreshold electrical stimulation to evaluate regenerative capacity of the cortex towards spreading depolarization (i.e. refractory period) (Fig. 3A). Electrical stimulation was delivered with fixed intensity and interval (800 μC every 6 min for 1 h). Paradigm 4: suprathreshold electrical stimulation with a large area of cortex exposed to the drug for measuring spreading depression amplitude (Fig. 4A). One recording electrode was placed inside and one outside of the drug bath large cranial window. An electrical pulse (0.4 mA, 640 ms) was delivered to the frontal cortex to induce a spreading depolarization as a baseline. Another spreading depression was induced 30 min after vehicle application, and again after another 30 min of vehicle or drug treatment. Time-matched spreading depolarization amplitudes recorded from both electrodes were compared between vehicle and drug-treated cortices. Paradigms 1 and 2 have been proven effective to predict therapeutic success of migraine prophylactic drugs (Ayata *et al.*, 2006), and the translational value of these paradigms has also been demonstrated in other studies (Eikermann-Haerter *et al.*, 2012*a*). Importantly, spreading depolarization frequency derived from Paradigm 1 seems to have concordance with the electrical spreading depolarization threshold to induce a single spreading depression in Paradigm 2 (Ayata, 2013). To investigate whether the downstream markers for neuroinflammation and trigeminovascular

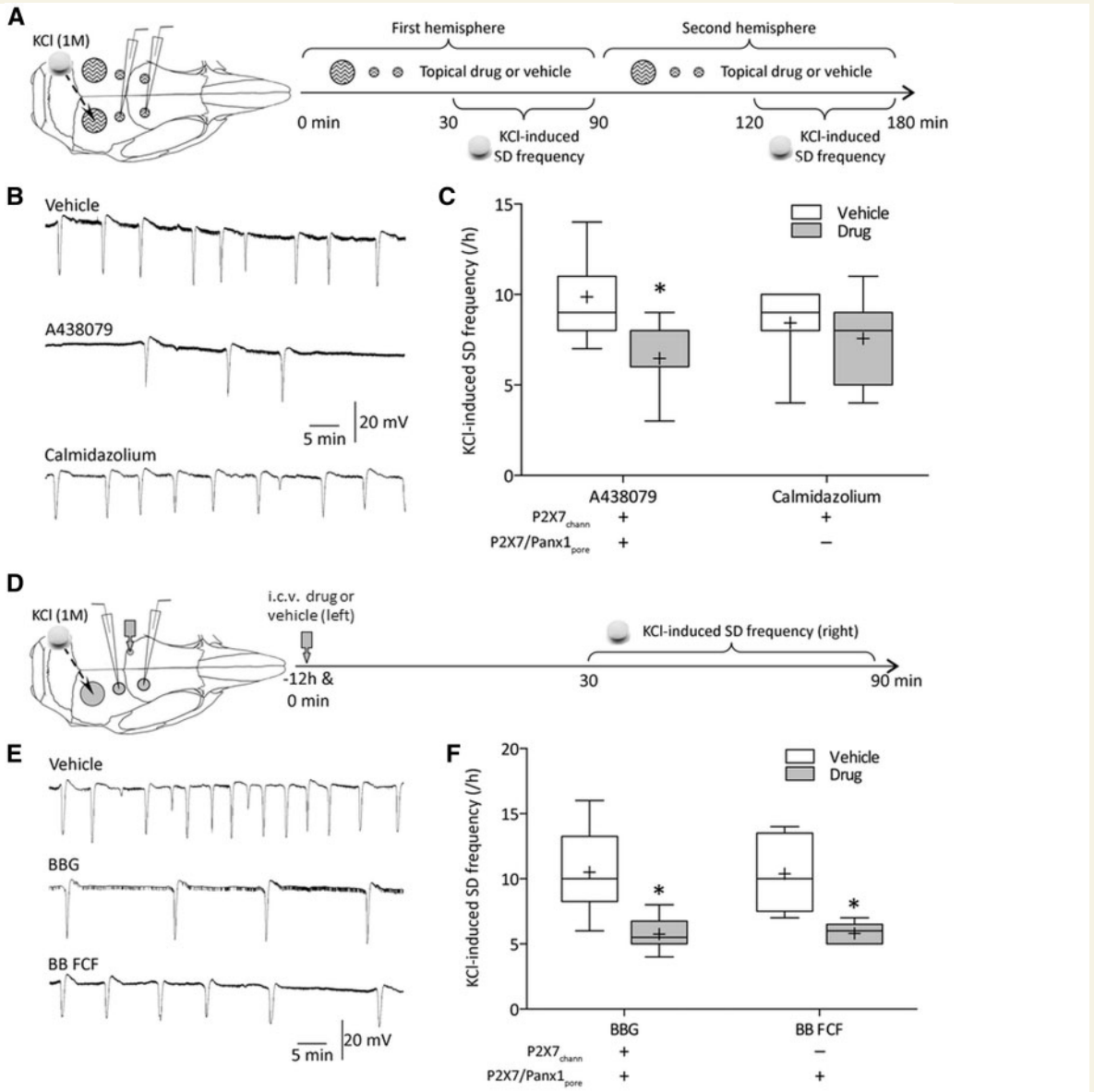

Figure 1 Topical or intracerebroventricular pharmacological inhibition of the 'P2X7-pannexin-1 pore complex' suppresses frequency of KCl-evoked spreading depolarization (SD) in rats. (**A**) After 30 min of pretreatment with drugs (A438079 or calmidazolium) or vehicles (0.9% normal saline or 1% DMSO), spreading depolarization frequency was measured during continuous topical application of 1 M KCl dissolved in drugs or vehicles. Both hemispheres were studied consecutively. (**B**) Representative intracortical microelectrode recordings show that the P2X7/PANX1$_{pore}$ inhibitor A438079 (4.38 mM) reduces KCl-evoked spreading depolarization frequency in rats. In contrast, selectively inhibiting the P2X7$_{chann}$ with calmidazolium (0.04 mM in 1% DMSO) did not affect spreading depolarization frequency. (**C**) Whisker–box plots show that A438079 (n = 15) but not calmidazolium (n = 7) reduces KCl-evoked spreading depolarization frequency in rats. (**D**) After pretreatment with drugs [Brilliant blue G (BBG) and Brilliant blue FCF (BB FCF)] or vehicles (0.9% NaCl), spreading depolarization frequency was measured during continuous topical application of 1 M KCl. (**E**) Representative intracortical microelectrode recordings show that the P2X7/PANX1$_{pore}$ inhibitors Brilliant blue G (5.85 mM) or Brilliant blue FCF (3.9 mM) reduced KCl-evoked spreading depolarization frequency in rats, when delivered intracerebroventricularly (i.c.v). (**F**) Whisker–box plots confirm that Brilliant blue G (n = 8) and Brilliant blue FCF (n = 5) reduce KCl-evoked spreading depolarization frequency in rats (whisker, full range; box, IQR; line, median; cross, mean; $^{*}P < 0.05$).

activation mentioned below are specific to spreading depression, we conducted experiments using topical 1 M NaCl solution (with the same osmolarity as KCl) (n = 5) and pinprick-induced spreading depolarizations (n = 5) for comparison. The expression of these markers in the cerebellum, where spreading depolarization does not propagate into, was investigated as well to show anatomical specificity. To investigate the mechanism of reduction in spreading depolarization amplitude in Paradigm 4, we studied the effect of P2X7/PANX1 antagonist A438079 on

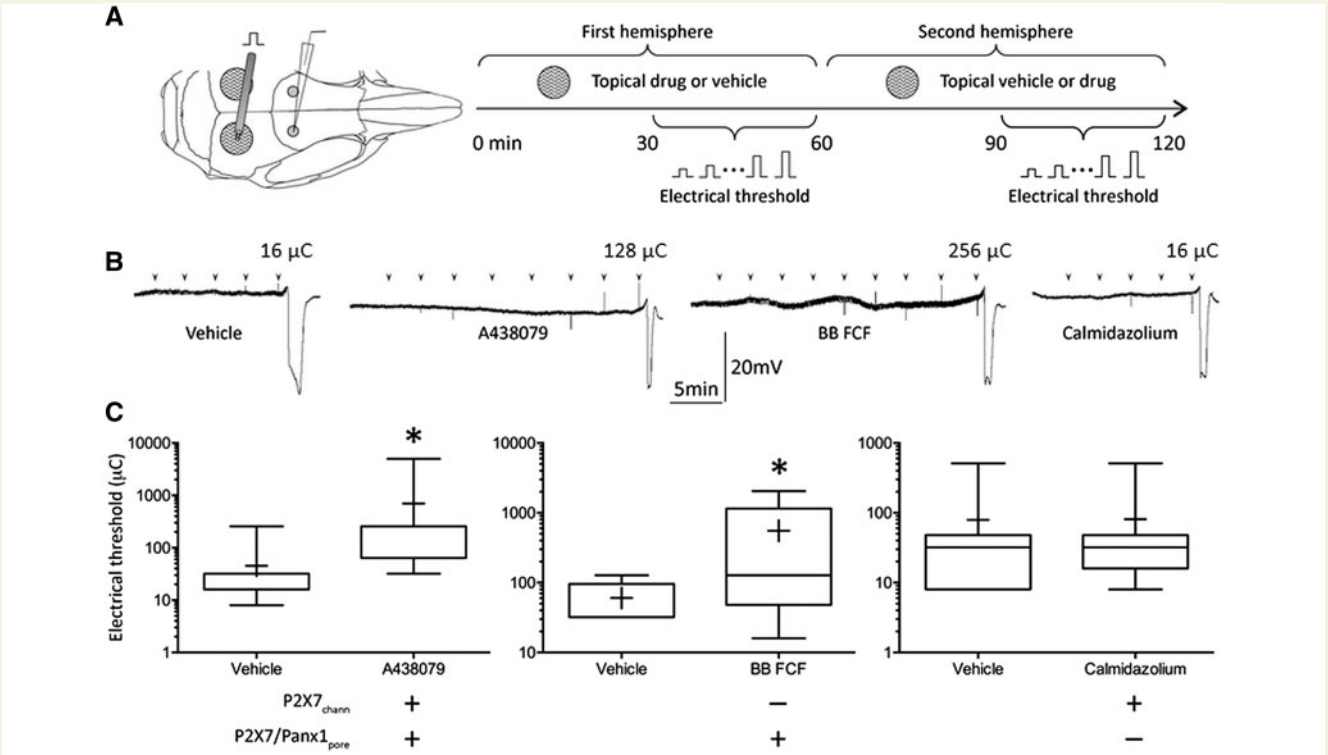

Figure 2 Pharmacological inhibition of the 'P2X7-pannexin-1 pore complex' increases the electrical threshold of spreading depolarization in mice. (**A**) Single-squared pulses of increasing duration and intensity were applied to the drug-bathed cortex every 4 min (1–2048 µC). (**B**) Representative tracings show that the P2X7/PANX1$_{pore}$ inhibitors A438079 (4.38 mM) and Brilliant blue FCF (BB FCF, 3.9 mM) elevate the electrical threshold for spreading depolarization. In contrast, selectively inhibiting the P2X7$_{chann}$ with calmidazolium (0.04 mM in 1% DMSO) did not affect electrical threshold. (**C**) Whisker–box plots show that A438079 and Brilliant blue FCF, but not calmidazolium, elevate the electrical threshold for spreading depolarization in mice (versus vehicle; $n = 9$ per group, Wilcoxon-signed ranked test; whisker, full range; box, IQR; line, median; cross, mean; $^{*}P < 0.05$). Note that the vertical axis is in log scale.

potassium release by simultaneously using a potassium-selective electrode and a micropipette for spreading depolarization recording ($n = 6$).

Quantitative polymerase chain reaction for *Il1b*

We performed quantitative reverse transcriptase polymerase chain reaction (qRT-PCR) on RNA isolated from a 2-mm wide (rostro-caudally) cortical strip of tissue between the occipital spreading depolarization induction site and the parietal recording site for mRNA of the pro-inflammatory cytokine *Il1b* gene as a direct downstream product of inflammasome activation (Karatas *et al.*, 2013; Walsh *et al.*, 2014), 4 h after KCl-induced spreading depolarization. The targeted cortex was pretreated with either drugs or vehicles for 30 min before spreading depolarization induction. To correct for the effect of spreading depolarization frequency on *Il1b* mRNA expression, we induced a fixed number of spreading depolarizations ($n = 6$ over 1 h with intermittent transient 1 M KCl topical application and immediate wash-out) in a new group of animals pre-treated with vehicle or drugs. Rats were deeply anaesthetized and transcardially perfused with phosphate-buffered saline (PBS). Brains, as well as trigeminal ganglion and trigeminal nucleus caudalis, were quickly collected, frozen with pre-chilled isopentane, bath-cooled with dry ice, and kept in a −80°C freezer. RNA extraction (Illustra RNAspin Mini RNA Isolation Kit, GE Healthcare), cDNA synthesis (with reverse transcription-PCR with SuperScript™ III First-Strand Synthesis System, Invitrogen), and real-time qPCR (TaqMan® Gene Expression Assays and TaqMan® Fast Advanced Master Mix; Life Technologies) were performed as reported previously (Li and Wang, 2000).

Western blot

Cox-2 (*Ptgs2*) and iNOS (inducible nitric oxide synthase, encoded by *Nos2*) expression in the cortical tissue (at the same location as *Il1b* qRT-PCR) and CGRP expression in the trigeminal ganglion ipsilateral to the spreading depolarization induction site were evaluated with western blot, after pretreatment with vehicle or A438079 ($n = 5$ per group) for 30 min at all craniotomy sites followed by induction of a fixed number of spreading depolarizations ($n = 6$ over 1 h). A sham control group ($n = 5$) with craniotomies but without spreading depolarization induction was used for comparison.

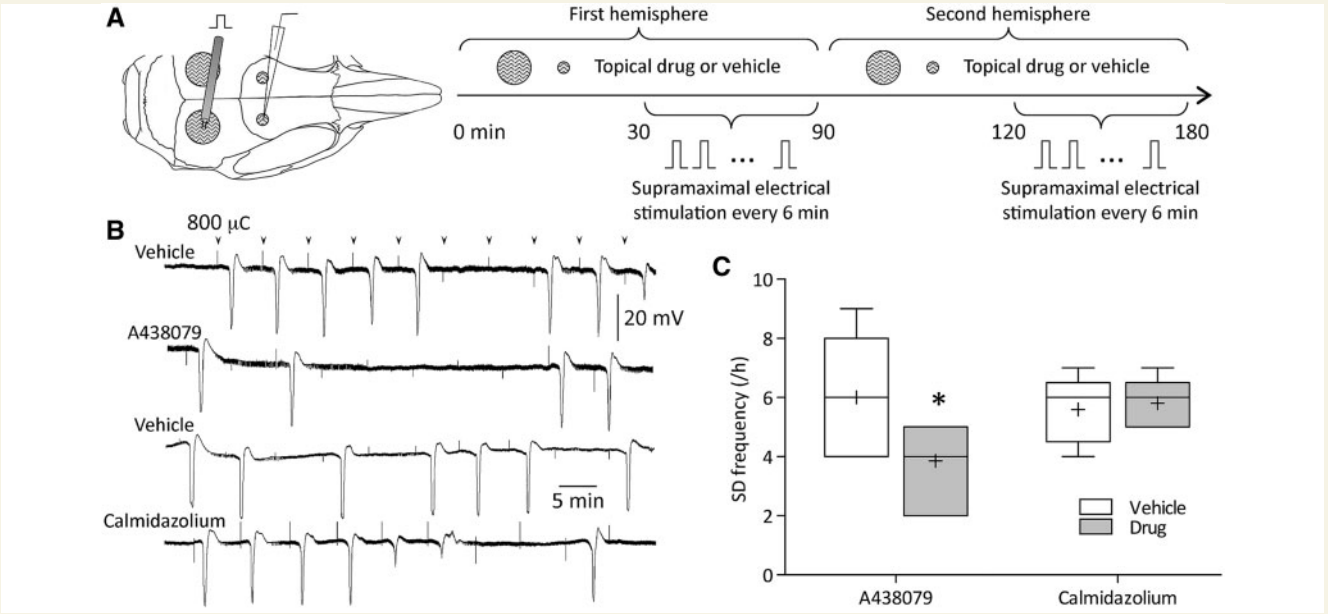

Figure 3 Pharmacological inhibition of the 'P2X7-pannexin-1 pore complex' suppresses regenerative capacity of the cortex towards spreading depolarization evoked by suprathreshold electrical stimulation in rats. (**A**) Repetitive supra-threshold electrical stimulation was used to evaluate regenerative capacity of the cortex towards spreading depolarization (i.e. refractory period). Electrical stimulation was delivered with fixed intensity and interval (800 μC every 6 min for 1 h), 30 min after topical treatment with drugs (A438079 or calmidazolium) or vehicles (0.9% normal saline or 1% DMSO). (**B**) Representative tracings show that the P2X7/PANX1$_{pore}$ inhibitor A438079 (4.38 mM) reduced repetitive electrical stimulation-evoked spreading depolarization frequency in rats. In contrast, selectively inhibiting the P2X7$_{chann}$ with calmidazolium (0.04 mM in 1% DMSO) did not affect spreading depolarization. (**C**) Whisker-box plots show that A438079 (n = 7), but not calmidazolium (n = 5), reduces spreading depolarization frequency during repetitive electrical stimulation in rats (whisker, full range; box, IQR; line, median; cross, mean; $^{*}P < 0.05$).

Brain tissues were collected 4 h after the beginning of spreading depolarization induction. Frozen tissues were resuspended and homogenized in phosphate buffer (pH 7.4; 0.06 M potassium phosphate, 1 mM EDTA). Protein concentrations were measured with the Bradford method. Aliquots of 7.5 mg protein each (as duplicates) were separated electrophoretically on 12% resolving polyacrylamide mini-gels using a Mini PROTEAN® II electrophoresis unit (Bio-Rad) and then quantitatively transferred to PVDF membranes. After incubation for 1 h in tris-buffered saline (TBS) containing 5% fat-free milk, the membranes were exposed to primary antibodies: anti-Cox-2 (1:1000, BD Transduction Laboratories), anti-iNOS (1:400, Abcam) and anti-CGRP (1:400, Abcam) at 4°C overnight. Subsequently, the membranes were incubated with horseradish peroxidase conjugated anti-rabbit IgG secondary antibody (1:3000, GE healthcare) for 1 h at room temperature. The content of targeted proteins was detected by enhanced chemiluminescence. Signals were normalized to β-actin (1:10 000, GeneTex).

Immunohistochemistry

Rats or mice were deeply anaesthetized and transcardially perfused with 4% paraformaldehyde after spreading depolarization studies. Brains were quickly removed, post-fixed in the same fixative overnight and cryoprotected in 30% sucrose solution for 2 days. Multiple 30-mm thick transverse sections were collected, incubated overnight with rabbit anti-c-Fos antibody (1:1000; Abcam), followed by 90 min with biotinylated goat anti-rabbit antibodies. Sections were rinsed before incubating for 90 min in streptavidin horseradish peroxidase solution and detection reagents. After mounting and dehydrating, expression of c-Fos in the trigeminal nucleus caudalis was determined by counting Fos-immunoreactive neurons in lamina I and II of trigeminal nucleus caudalis from five sections of the cervical spinal cord and five sections from the caudal medulla. The data were averaged and reported as the number of cells per section. To investigate whether spreading depression-induced upregulation of neuroinflammatory markers is associated with cellular injury, we evaluated the uptake of intraperitoneally injected propidium iodide, a marker of cellular injury/death, in cortical neurons 30 min after spreading depolarization in comparison with a positive control after controlled cortical impact traumatic brain injury. Cortices at the spreading depolarization induction site (i.e. KCl application site) and 2 mm remote from the spreading depolarization induction site were collected for analysis.

Behavioural testing

Open field test and pole test were used to assess behaviour over 3 h after systemic administration of P2X7 antagonist A438079 in awake mice as described previously (Balkaya

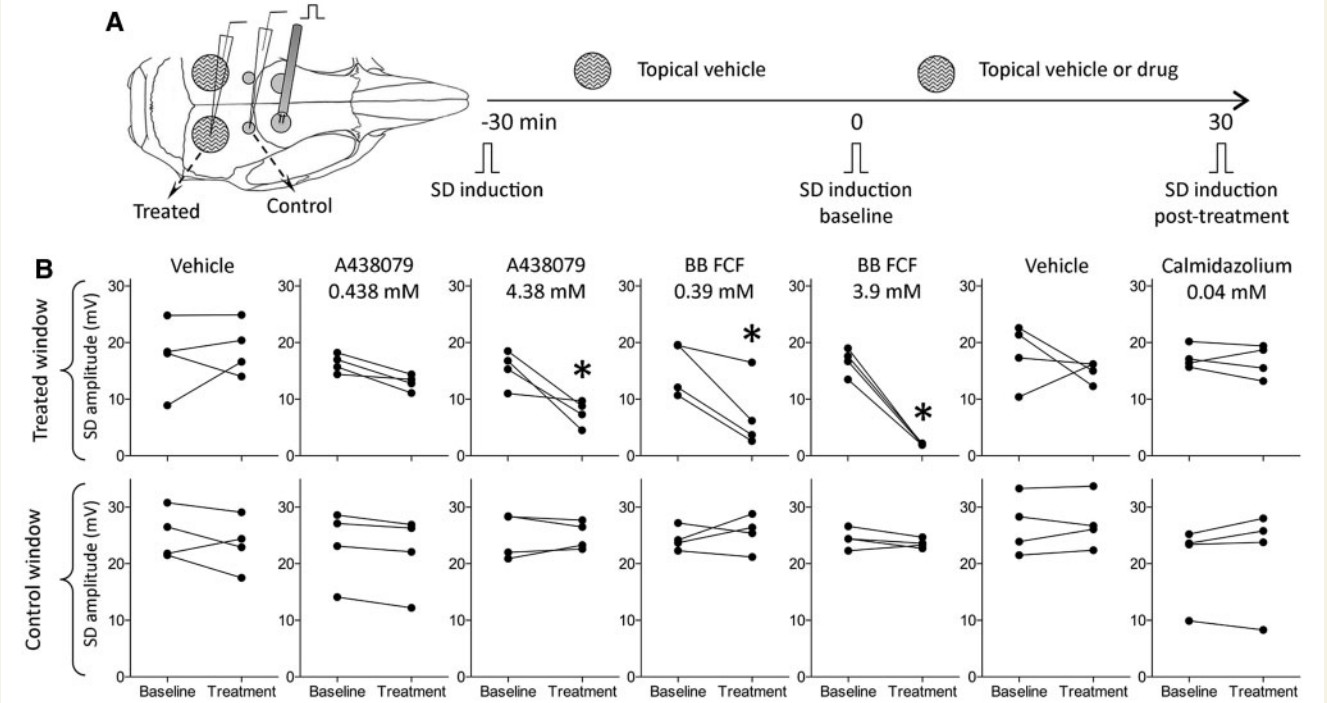

Figure 4 Pharmacological inhibition of the 'P2X7-pannexin-1 pore complex' reduces the amplitude of spreading depolarization. (**A**) One recording electrode was placed inside a 3 mm drug-bathed cranial window, and another one outside the window as a control. A supra-threshold electrical pulse (0.4 mA, 640 ms) was delivered to the frontal cortex to induce a spreading depolarization (SD) as a baseline. Another spreading depolarization was induced 30 min after vehicle application, and again after another 30 min of vehicle or drug treatment. Time-matched spreading depolarization amplitudes recorded from both electrodes were compared between vehicle and drug-treated cortices. (**B**) Topical administration of the P2X7/PANX1$_{pore}$ inhibitor A438079 (0.438–4.38 mM) or Brilliant blue FCF (BB FCF; 0.39–3.9 mM) reduced spreading depolarization amplitude within the treatment window, with a dose-response relationship (*top row*), whereas spreading depolarization amplitudes recorded outside the treatment window were unaffected (*bottom row*) ($n = 4$ per group) ($^{*}P < 0.001$, two-way repeated measures ANOVA with *post hoc* Bonferroni test). In contrast, the P2X7$_{chann}$ inhibitor calmidazolium had no effect on spreading depolarization amplitude either in the treated or control window ($n = 4$).

and Endres, 2010). In brief, open field test was performed for 30 min, followed by the pole test 5 min later. These two tests were repeated in the second and third hour after intraperitoneal injection of A438079. With a cross-over design, mice initially treated with vehicle received A438079 1 month later (and vice versa), and behaviour was reassessed with the same protocol ($n = 4$ mice per drug).

Statistical analysis

Values are reported as mean ± standard deviation (SD), mean ± standard error of the mean (SEM) or median and interquartile range (IQR), as indicated. For parametric variables including spreading depolarization frequency and systemic physiology, one-way ANOVA, Student's *t*-test or paired *t*-test were used for comparison as appropriate. For non-parametric variables including spreading depression electrical threshold, *Il1b* mRNA, relative expression of Cox-2, iNOS, or CGRP, and c-Fos immunoreactive cells, either the Kruskal-Wallis test with *post hoc* Dunn's multiple comparison test or the Mann-Whitney U-test was used for comparisons of non-paired data; the Wilcoxon signed-rank test was used for paired data. For comparison of a dependent variable with at least two time points from multiple groups such as spreading depolarization amplitude or frequency in different strains of mice upon pharmacological intervention, two-way repeated measures ANOVA with *post hoc* Bonferroni test was performed. The Pearson's correlation test was used to study the relationship between spreading depolarization frequency and *Il1b* expression, as well as that between potassium concentration and spreading depolarization amplitude. All calculated *P*-values were two-tailed, and $P < 0.05$ was considered significant. Statistical analysis was performed using GraphPad Prism 5 (GraphPad Software, La Jolla, CA) and IBM SPSS Statistics version 23 (IBM, Armonk, NY).

Results

Pharmacological inhibition of the P2X7/PANX1$_{pore}$ suppresses spreading depolarization

Drugs targeting both P2X7$_{chann}$ and P2X7/PANX1$_{pore}$ (Brilliant blue G and A438079) or selectively the P2X7/

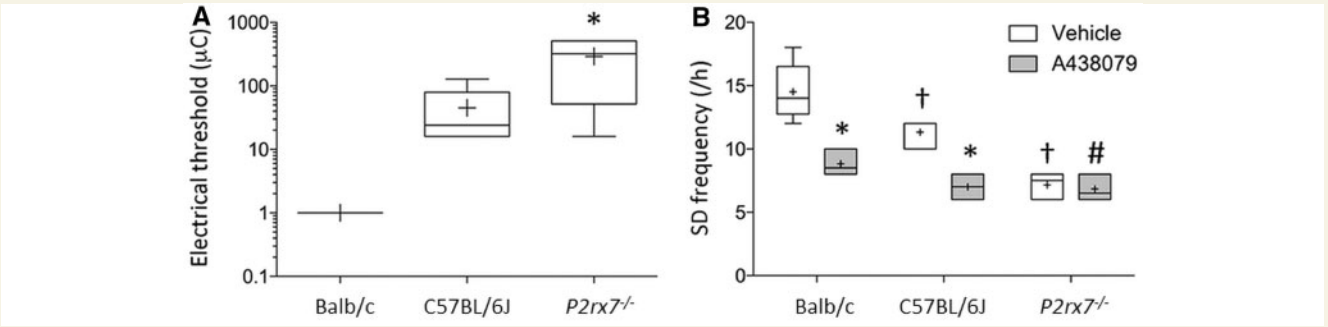

Figure 5 Genetic impairment (by a spontaneous mutation or knock-out) of *P2rx7* suppresses susceptibility to spreading depolarization. (**A**) Electrical threshold of spreading depolarization was lowest in Balb/c mice with intact P2X7/PANX1$_{pore}$ function, followed by C57BL/6J *P2rx7*^{P451L} mice with partially impaired pore formation due to a loss-of-function mutation of *P2rx7*. *P2rx7* knockout mice exhibited the highest spreading depolarization threshold ($n = 6$ per group) ($P = 0.001$ for Kruskal-Wallis test; $^{*}P < 0.05$, *post hoc* Dunn's test). (**B**) Spreading depolarization frequency upon continuous KCl stimulation was highest in Balb/c mice, followed by C57BL/6J *P2rx7*^{P451L} and then *P2rx7*$^{-/-}$ with the lowest frequency. Pharmacological pore inhibition with the P2X7 antagonist A438079 (4.38 mM, topical application) reduced spreading depolarization frequency in Balb/c and C57BL/6J *P2rx7*^{P451L} mice, but not in *P2rx7*$^{-/-}$ mice (whisker, full range; box, IQR; line, median; cross, mean; ($^{\dagger}P < 0.01$ versus Balb/c; $^{*}P < 0.001$, $^{\#}P > 0.05$, versus vehicle treated cortex; two-way ANOVA with *post hoc* Bonferroni's test). Note that the vertical axis of spreading depolarization threshold is expressed as log scale.

PANX1$_{pore}$ (Brilliant blue FCF) reduced spreading depolarization susceptibility. The frequency of KCl-induced repetitive spreading depolarizations in 1 h decreased by 34% ($P < 0.001$, paired *t*-test) in rats that were subjected to topical application of the P2X7/PANX1$_{pore}$ inhibitor A438079 (4.38 mM) but not the P2X7$_{chann}$ inhibitor calmidazolium (0.04 mM) ($P = 0.341$, paired *t*-test) (Fig. 1). Intracerebroventricular injection of the other two P2X7/PANX1$_{pore}$ inhibitors Brilliant blue G (5.85 mM) and Brilliant blue FCF (3.9 mM) also reduced KCl-evoked spreading depolarization frequency in rats by ~44% in comparison with vehicles ($P = 0.002$ for Brilliant blue G and $P = 0.026$ for Brilliant blue FCF, Student's *t*-test) (Fig. 1). Similar to topical treatment, intracerebroventricular injection with the P2X7$_{chann}$ inhibitor calmidazolium (1.67 mM) had no effect on spreading depolarization frequency ($P = 0.339$, Student's *t*-test). This inhibitory effect of P2X7/PANX1$_{pore}$ on spreading depolarization susceptibility was consistent across species. The electrical spreading depolarization threshold increased by 4- to 16-fold (median) in mice upon topical treatment with the P2X7/PANX1$_{pore}$ inhibitors A438079 and Brilliant blue FCF, but not the P2X7$_{chann}$ inhibitor calmidazolium ($P = 0.008$ for A438079, $P = 0.044$ for Brilliant blue FCF, and $P = 0.157$ for calmidazolium, Wilcoxon signed-rank test) (Fig. 2)—Brilliant blue G was not used in mice because it is a rat selective antagonist that only acts on mice P2X7 receptor with sufficiently long incubation time *in vitro* (Donnelly-Roberts *et al.*, 2009). A438079 also inhibits KCl-evoked spreading depolarization frequency by ~30–35% in wild-type C57BL/6J mice, either administered systemically (300 µmol/kg, intraperitoneal) (7.4 ± 0.5/h versus 10.8 ± 1.1/h, $n = 10$ per group, $P = 0.007$; Student's *t*-test) or topically (4.38 mM) (8.0 ± 1.5/h versus 11.3 ± 1.8/h, $n = 8$, $P = 0.002$; paired *t*-test) in comparison with vehicles (Supplementary Fig. 1). Systemic intraperitoneal drug administration of A438079 (300 µmol/kg) also tended to reduce propagation speed (4.2 ± 0.7 versus 3.2 ± 0.7 cm/min, $P = 0.057$). The spreading depolarization frequency in the homozygous *Cacna1a*^{R192Q} mutants, which exhibit genetically enhanced spreading depolarization susceptibility, was also inhibited by A438079 (4.38 mM) to a similar extent (10.0 ± 1.8/h versus13.7 ± 1.0/h, $n = 6$ per group, $P = 0.003$; paired *t*-test).

To assess the regenerative capacity of the cortex towards spreading depolarization, we performed repetitive suprathreshold electrical stimulation of the cortex. A438079 (4.38 mM) again reduced spreading depolarization frequency by approximately one-third during repetitive electrical stimulation in rats (3.9 ± 1.3/h versus 6.0 ± 2.1/h, $P = 0.032$; paired *t*-test) (Fig. 3), suggesting a prolonged refractory period of the brain towards spreading depolarization after P2X7/PANX1$_{pore}$ inhibition. In contrast, topical treatment with P2X7$_{chann}$ inhibitor calmidazolium (0.04 mM) had no significant effects when compared with vehicles (5.8 ± 0.8 versus 5.6 ± 1.1, $P = 0.749$; paired *t*-test). Within the cortex exposed to the P2X7/PANX1$_{pore}$ inhibitors A438079 (0.44–4.38 mM) and Brilliant blue FCF (0.39–3.9 mM) directly, spreading depolarization amplitudes were reduced by 35–90% in a dose-dependent fashion, whereas the P2X7$_{chann}$ inhibitor calmidazolium (0.04 mM) did not inhibit the amplitude of spreading depolarization (Fig. 4). The amplitude of spreading depolarization correlated with extracellular potassium concentration when pretreated with A438079 ($n = 6$, $r = 0.990$, $P < 0.001$), suggesting that reduced spreading depolarization amplitude might be the consequence of inhibition of K^{+} release by P2X7/PANX1 antagonism. Notably, inhibiting the coupling of P2X7 to PANX1 by intraperitoneally administered Src kinase inhibitor PP2 (0.1 mM) also reduced spreading depolarization frequency by 30% in Balb/c mice (vehicle versus PP2: 15.5 ± 1.4 versus 11.2 ± 1.6/h, $P = 0.004$, Student's *t*-test).

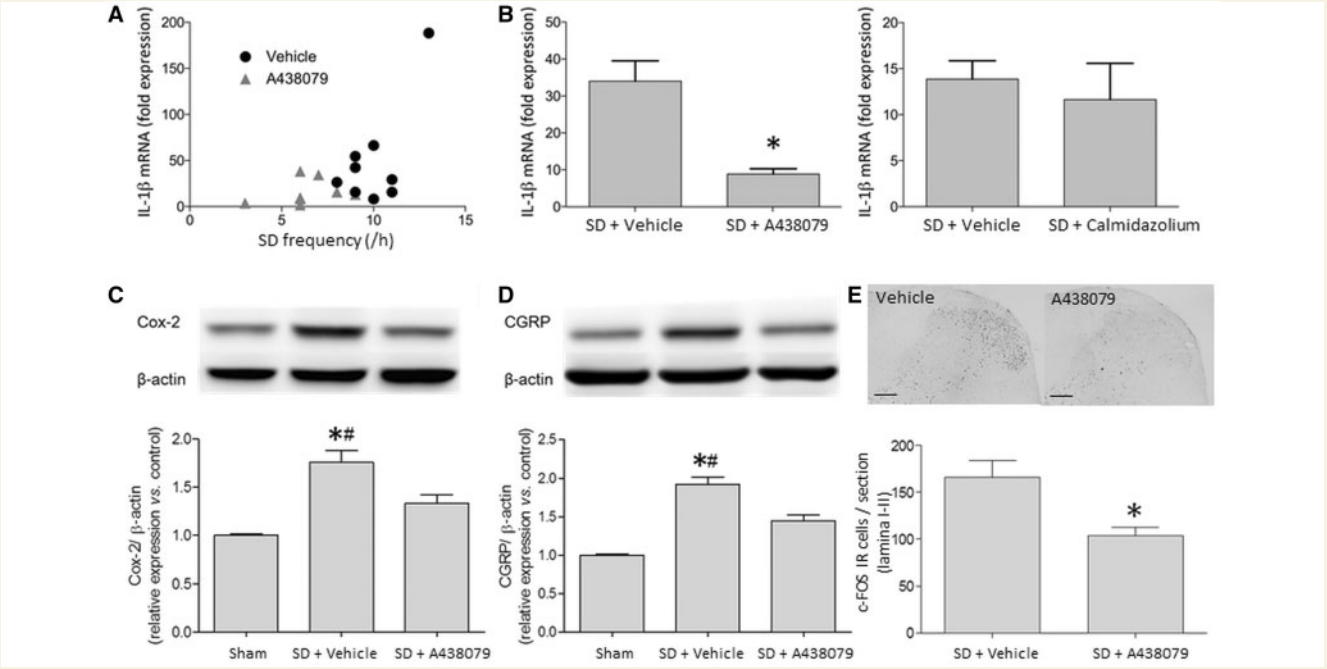

Figure 6 P2X7 antagonists suppress spreading depolarization-induced cortical inflammation and trigeminovascular activation. (**A**) Spreading depolarization upregulates the expression of cortical *Il1b* mRNA, with a trend of correlation with total number of spreading depolarizations. (**B**) After eliminating the confounding effect of spreading depolarization frequency by inducing a fixed number of spreading depolarizations (6/h) in a new cohort of animals, the P2X7/PANX1$_{pore}$ inhibitor A438079 (4.38 mM) inhibits *Il1b* mRNA upregulation in comparison with vehicle (0.9% normal saline) (n = 6 per group, P = 0.002), whereas the P2X7$_{chann}$ inhibitor calmidazolium (0.04 mM) had no effect on *Il1b* mRNA expression in comparison with vehicle (1% DMSO) (n = 6 per group; P = 0.665). (**C**) Western blot analysis of spreading depolarization-induced cortical Cox-2 expression in vehicle- and A438079-pretreated animals in comparison with sham controls (n = 5 per group). Band intensities were quantified by densitometry and are indicated as fold change relative to that of the sham control group. Cox-2 expression increased after spreading depolarization induction ($^{*}P$ = 0.008 versus sham controls), which was suppressed by pretreatment with A438079 (4.38 mM) ($^{\#}P$ = 0.016). (**D**) Western blot analysis of spreading depolarization-induced CGRP expression in trigeminal ganglion in vehicle- and A438079-pretreated animals in comparison with sham controls (n = 5 per group). Band intensities were expressed as fold change relative to that of the sham control group. Densitometric analysis showed elevated CGRP expression after spreading depolarization induction ($^{*}P$ = 0.008 versus sham controls), which was suppressed by pretreatment with A438079 (4.38 mM) ($^{\#}P$ = 0.008). (**E**) The *upper panel* illustrates representative images of c-Fos immunoreactive cells in trigeminal nucleus caudalis (coronal section, 3 mm caudal from obex) following spreading depolarizations in vehicle and A438079 pretreated animals (Scale bars = 200 μm). *Lower panel* shows that after A438079 (4.38 mM) treatment, immunoreactivity of c-Fos neurons was significantly lower in comparison with controls (n = 5 per group; $^{*}P$ = 0.016). Mann-Whitney U-test was used for all analyses. Error bars indicate SEM.

Genetic loss of P2X7/PANX1$_{pore}$ function suppresses spreading depolarization

To dissect the mechanism underlying spreading depolarization suppression by P2X7/PANX1$_{pore}$ inhibitors further, we tested spontaneous and engineered genetic mouse models. The commonly used wild-type strain C57BL/6J carries a spontaneous P451L missense mutation in the *P2rx7* gene (*P2rx7*^{P451L}), which partially impairs P2X7/PANX1$_{pore}$ formation by altering the Src tyrosine kinase binding site in the carboxyl terminal, thereby causing partial loss of P2X7/PANX1$_{pore}$ function (Adriouch *et al.*, 2002; Sorge *et al.*, 2012). In contrast, the wild-type strain Balb/c carries a completely functional *P2rx7* gene. Consistent with the data obtained using pharmacological inhibitors, C57BL/6J mice (with partial loss of P2X7/PANX1$_{pore}$ function) showed lower spreading depolarization susceptibility compared to Balb/c mice (with normal P2X7/PANX1$_{pore}$ function) (Fig. 5). Susceptibility to spreading depolarization was even lower in *P2rx7*$^{-/-}$ knockout mice (B6.129P2-*P2rx7*^{tm1Gab}/J) with ablation of P2X7 function, and could not be further reduced by the P2X7$_{chann}$ and P2X7/PANX1$_{pore}$ inhibitor A438079, confirming target specificity in this experimental spreading depolarization paradigm (Fig. 5B).

Pharmacological blockade of the P2X7/PANX1$_{pore}$ inhibits neuroinflammation after spreading depolarization

Our experiments show that spreading depolarization upregulates cortical *Il1b* mRNA. Importantly, the *Il1b* mRNA

expression level correlated with the number of spreading depressions in treated cortex ($r = 0.669$, $P = 0.049$) (Fig. 6A). When a fixed number of spreading depolarizations was evoked ($n = 6$ over 1 h) to correct for the effect of spreading depression frequency on *Il1b* mRNA expression, inhibition of the P2X7/PANX1$_{pore}$ with A438079 (4.38 mM) reduced spreading depolarization-induced cortical *Il1b* mRNA expression by 77%. In contrast, selective inhibition of the P2X7$_{chann}$ function with calmidazolium (0.04 mM) had no effect (Fig. 6B), indicating that suppression of spreading depolarization-induced *Il1b* mRNA upregulation was due to inhibition of the P2X7/PANX1$_{pore}$, and not the P2X7$_{chann}$. Spreading depolarization upregulated cortical Cox-2 expression (1.75-fold compared to sham, $P = 0.008$), which was partially prevented by the P2X7/PANX1$_{pore}$ inhibitor A438079 with a reduction of relative expression to 1.33-fold ($P = 0.016$; Mann-Whitney U-test) (Fig. 6C). Similarly, spreading depolarization upregulated cortical iNOS expression (1.35-fold compared to sham, $P = 0.008$), which was attenuated by the P2X7/PANX1$_{pore}$ inhibitor A438079 with a reduction of relative expression ($P = 0.008$; Mann-Whitney U-test; Supplementary Fig. 2).

Pharmacological blockade of the P2X7/PANX1$_{pore}$ inhibits trigeminovascular activation after spreading depolarization

To investigate whether P2X7-PANX1 blockade prevents spreading depolarization-induced activation of the trigeminovascular system, we examined CGRP expression at the trigeminal ganglion and c-Fos expression at the trigeminal nucleus caudalis after spreading depolarization. Spreading depression upregulated CGRP expression at the trigeminal ganglion by 1.92-fold compared to sham, which was partially suppressed to 1.45-fold by pretreatment with the P2X7/PANX1$_{pore}$ inhibitor A438079 ($P = 0.008$; Mann-Whitney U-test) (Fig. 6D). In addition, A438079 pretreatment reduced spreading depolarization-induced c-Fos expression in the trigeminal nucleus caudalis in comparison with controls (median: 95.7 versus 171.8 cells/section, $P = 0.016$; Mann-Whitney U-test) (Fig. 6E).

Specificity of spreading depolarization on neuroinflammation and trigeminovascular activation

To investigate whether the downstream markers for neuroinflammation and trigeminovascular activation mentioned above are specific to spreading depression, we conducted experiments using pinprick-induced spreading depolarization ($n = 5$), and found a similar upregulation of markers. In contrast, topical 1 M NaCl solution (with the same osmolarity as KCl) ($n = 5$) did not induce spreading depolarization or affect expression of markers. Spreading depolarization-induced expression of markers was anatomically specific because neither IL-1β, Cox-2, CGRP nor c-Fos immunoreactivity was upregulated in cerebellum, where spreading depolarization does not propagate into following cortical induction of spreading depolarization (Supplementary Fig. 3). Expression of these markers was unlikely attributed to permanent cellular damage because neither the spreading depression induction site nor remote cortical regions showed uptake of propidium iodide 30 min after induction of spreading depolarization ($n = 3$) (Supplementary Fig. 4).

Pharmacological blockade of the P2X7/PANX1$_{pore}$ does not affect gross behaviours in mice

Systemic intraperitoneal administration of A438079 (300 μmol/kg) did not cause gross behavioural impairment in open-field test and pole test in mice (Supplementary Fig. 5), while it reduced spreading depolarization frequency as effectively as topical administration of the same drug (Supplementary Fig. 1).

Discussion

Here we show for the first time that pharmacological inhibition or genetic loss of P2X7 as part of the P2X7/PANX1$_{pore}$ suppresses spreading depolarization and, independently, its downstream inflammatory effects and trigeminovascular activation. Impaired coupling of P2X7 with PANX1 inhibits spreading depolarization to a similar degree as pharmacological inhibition or genetic ablation of P2X7/PANX1$_{pore}$ function. Pharmacological inhibition of the P2X7/PANX1$_{pore}$ suppresses spreading depolarization in wild-type rats and mice as well as in FHM1 transgenic mice with an increased spreading depolarization susceptibility due to a gain of function of mutated $Ca_v2.1$ channels (van den Maagdenberg *et al.*, 2004; Eikermann-Haerter *et al.*, 2009). In contrast, selective pharmacological inhibition of the P2X7$_{chann}$ did not affect spreading depolarization threshold or frequency. Notably, systemic drug administration of A438079 was similarly effective, without causing gross neurological dysfunction, as reported in clinical trials in patients with rheumatoid arthritis (Keystone *et al.*, 2012; Stock *et al.*, 2012). The fact that spreading depolarizations were attenuated upon different stimulation protocols and in different species underscores the robustness and importance of P2X7/PANX1$_{pore}$ inhibitors in suppressing initiation and propagation of spreading depolarization, as well as prolonging the refractory period after spreading depolarization (Pietrobon and Moskowitz, 2014). Our findings provide a novel avenue for targeting the P2X7/PANX1$_{pore}$ to suppress spreading depolarization and subsequent neuroinflammation, with relevance for

diseases associated with spreading depolarization, such as migraine (Chen and Ayata, 2016).

Spreading depolarization has recently been reported to induce PANX1 pore formation, while the non-specific PANX1 inhibitor carbenoxolone did not suppress spreading depression when delivered intraventricularly (Karatas *et al.*, 2013). Our study shows that inhibition of the P2X7/PANX1$_{pore}$ suppresses spreading depolarization, while selective pharmacological targeting of the P2X7$_{chann}$ does not affect spreading depolarization. Impaired function of the P2X7/PANX1$_{pore}$ may reduce spreading depolarization-induced release of K^+ (Buisman *et al.*, 1988), glutamate (Cervetto *et al.*, 2012), and/or pro-inflammatory cytokines (Pusic *et al.*, 2014) that facilitate spreading depolarization. In fact, *P2rx7*$^{-/-}$ mice that do not form functional pore complexes (Salas *et al.*, 2013) show no release of ^{3}H-glutamate (Csolle *et al.*, 2013) and no increased expression of *Il1b* (Clark *et al.*, 2010) in response to ATP. The lack of effect of the P2X7 antagonist A438079 on spreading depolarization in *P2rx7*$^{-/-}$ mice, at the same dose that effectively suppressed spreading depolarization in wild-type and FHM1 mice to *P2rx7*$^{-/-}$ levels, underscores the critical role of P2X7 in determining spreading depolarization susceptibility.

Spreading depolarization induces inflammatory cascades in neurons and glial cells, and was shown to activate the trigeminovascular system in animals (Moskowitz *et al.*, 1993; Bolay *et al.*, 2002; Karatas *et al.*, 2013). Spreading depolarization is thought to underlie aura and probably headache (evidence for the latter comes from experimental animal studies), while exacerbating neuronal injury and infarct progression during stroke (Eikermann-Haerter *et al.*, 2012*b*). The pro-inflammatory cytokine IL-1β may mediate part of the detrimental effects of spreading depression in migraine and stroke (Lambertsen *et al.*, 2012) because it activates and increases mechanosensitivity of meningeal nociceptors (Zhang *et al.*, 2012), stimulates the release of prostaglandin E2/CGRP in rat trigeminal ganglia cells (Neeb *et al.*, 2011), and exacerbates ischaemic brain damage in middle cerebral artery occlusion models in rats (Yamasaki *et al.*, 1995). Our study reveals that spreading depression-induced *Il1b* upregulation correlates with the cumulative number of spreading depolarizations. Hence, strategies to suppress spreading depolarization may become important therapeutic tools in migraine and perhaps stroke. The detrimental effects of spreading depolarization and inflammasome activation in ischaemic stroke are well known, and one can speculate that our finding of P2X7 antagonism suppressing spreading depolarization and spreading depolarization-evoked inflammasome activation might provide one possible explanation for the protective effect of P2X7 inhibition in stroke models. We show that inhibition of the P2X7/PANX1$_{pore}$, but not the P2X7$_{chann}$, suppresses spreading depolarization-induced upregulation of *Il1b*. Consistent with this finding, the P2X7/PANX1$_{pore}$ antagonist Brilliant blue G has been reported to suppress caspase-1-induced maturation of IL-1β/IL-18 after subarachnoid haemorrhage (Chen *et al.*, 2013). In addition, we found that cortical expression of iNOS and Cox-2, other inflammatory markers, was increased in response to spreading depolarization, consistent with the report by Karatas *et al.* (2013) when using a different assay. Pretreatment with the P2X7/PANX1$_{pore}$ inhibitor effectively abolished spreading depolarization-evoked cortical iNOS and Cox-2 upregulation, supporting a role for the P2X7/PANX1$_{pore}$ in spreading depolarization-mediated neuroinflammation. In parallel with the inhibition of cortical neuroinflammation, spreading depolarization-evoked CGRP expression at the trigeminal ganglion and c-Fos expression at the trigeminal nucleus caudalis were inhibited by P2X7/PANX1$_{pore}$ blockade, strengthening the potential role of the P2X7/PANX1$_{pore}$ in trigeminovascular activation. Recently, it was reported that Brilliant blue G, an inhibitor of the P2X7 channel and pore form, inhibits nitroglycerin-induced thermal hyperalgesia in mice as well as c-Fos upregulation in the trigeminal nucleus caudalis (Goloncser and Sperlagh, 2014). Other recent studies showed that P2X7 receptors are expressed in trigeminal satellite glial cells responsible for the pro-nociceptive effects of ATP (Yegutkin *et al.*, 2016), and that Brilliant blue G inhibits c-Fos expression in the trigeminal nucleus caudalis after orofacial formalin stimulation (Bohar *et al.*, 2015). These findings, together with ours, suggest that the role of P2X7 in migraine pathophysiology might be multi-faceted by acting at different levels involved in migraine pathophysiology.

Our study has several limitations. First, the use of genetic mutants allows target-specific study, but may encounter the possibility of developmental compensation. However, both pharmacological P2X7/PANX1$_{pore}$ inhibitors and genetic ablation of the P2X7 receptor similarly suppress spreading depolarization, reducing the potential negative impact of this contention. Second, additional pathways not involving Src kinase and PANX1 could be affected by P2X7/PANX1$_{pore}$ inhibitors (Iglesias *et al.*, 2008). Regardless, our findings suggest a predominant role for the P2X7-dependent pathway in modulating spreading depolarization susceptibility because selective inhibitors of the P2X7/PANX1$_{pore}$ and Src kinase suppressed spreading depolarization to a similar extent. In addition, although it is still debated whether the pore involves PANX1 or not (Alberto *et al.*, 2013), our results along with those of others (Pelegrin and Surprenant, 2006; Locovei *et al.*, 2007; Iglesias *et al.*, 2008; Gulbransen *et al.*, 2012; Poornima *et al.*, 2012; Di Cesare Mannelli *et al.*, 2015; Pan *et al.*, 2015) are more in favour of a pore complex formed by the coupling of P2X7 to PANX1. Third, measuring *Il1b* mRNA expression is not equivalent to measuring IL-1β protein. However, *IL1B* is a transcriptionally-regulated gene, and the level of its transcript correlates well with the level of protein (Rioja *et al.*, 2004; Li *et al.*, 2008; Zhang *et al.*, 2008). There is concern that there might be non-specific activation of genes involved in cell injury following spreading depolarization; however, a recent study

showed that after spreading depolarization immune system-related genes are selectively upregulated (Eising *et al.*, 2016). To provide more evidence of selective activation of inflammatory pathways, we evaluated the expression of another inflammatory marker, Cox-2, in the cortex following spreading depolarization by western blot. We demonstrated that upregulation of Cox-2 can similarly be inhibited with A438079 pretreatment. In addition, we demonstrated increased expression of CGRP in the trigeminal ganglion, and c-Fos expression in the trigeminal nucleus caudalis, augmenting the potential relevance of our findings for migraine pathophysiology. Fourth, the specificity of calmidazolium on P2X7 and Brilliant blue FCF on PANX1 has been well established *in vitro*, but not yet sufficiently *in vivo*; however, the significant effect of Brilliant blue FCF on spreading depolarization susceptibility was similar to that of A438079 and Brilliant blue G, suggesting that our findings were unlikely to be false positive or due to non-specific targeting. The lack of an effect of calmidazolium on spreading depolarization susceptibility despite equivalently potent or higher dosing than A438079 supports a true finding. Finally, there might be localized damage to the cortex with rippling effects at some distance after prolonged exposure to topical KCl, although we used cortical tissue as far as 2 mm away from the stimulation site. Despite these limitations, various studies have used very similar approaches to investigate downstream effects of spreading depolarization (Karatas *et al.*, 2013; Eising *et al.*, 2016). In addition, we did not find evidence for cellular damage secondary to topical KCl because no propidium iodide uptake was observed both at the KCl application site and remote from it (Supplementary Fig. 4).

In conclusion, our data show that the P2X7/PANX1$_{pore}$ is an important determinant of spreading depolarization susceptibility, as well as activation of the inflammasome and trigeminovascular system, in response to spreading depolarization. P2X7/PANX1$_{pore}$ inhibitors provide a promising and well-tolerated candidate for therapeutic suppression of spreading depolarization and neuroinflammation, with relevance for neurological disorders associated with spreading depolarization, such as migraine and stroke. Future studies are needed to further investigate clinical implications of our findings.

Acknowledgements

We would like to express our gratitude to Dr Jiin-Cherng Yen and Tzu-Ting Liu, Institute of Pharmacology, National Yang-Ming University, Taipei, Taiwan, for technical support of experiments.

Funding

This work was supported by the American Heart Association (10SDG2610275 to K.E.H.); the Massachusetts General Hospital (Claflin Distinguished Award to K.E.H.); the Ministry of Science and Technology of Taiwan (MOST 104-2314-B-075 -006 -MY3 to S.P.C), Taipei Veterans General Hospital (V104C-174 to S.P.C), Taipei Veterans General Hospital-National Yang-Ming University Excellent Physician Scientists Cultivation Program (No.102-V-A-001 and No. 104-V-B-035 to S.P.C.); and the Vivian W. Yen Neurological Foundation (2013 research grant to S.P.C.) and by the Center for Medical Systems Biology (CMSB) established by the Netherlands Genomics Initiative/Netherlands Organization for Scientific Research (project No. 050–060-409, A.M.J.M.v.d.M.).

Supplementary material

Supplementary material is available at *Brain* online.

References

Adinolfi E, Cirillo M, Woltersdorf R, Falzoni S, Chiozzi P, Pellegatti P, et al. Trophic activity of a naturally occurring truncated isoform of the P2X7 receptor. FASEB J 2010; 24: 3393–404.

Adriouch S, Dox C, Welge V, Seman M, Koch-Nolte F, Haag F. Cutting edge: a natural P451L mutation in the cytoplasmic domain impairs the function of the mouse P2X7 receptor. J Immunol 2002; 169: 4108–12.

Akaike N, Himori N. Excitatory amino acid-elicited tonic convulsions in mice and N-methyl-D-aspartate receptor activation: role of Ca(2+) influx and involvement of intracellular Ca(2+)-dependent biochemical processes. Pharmacology 2002; 66: 136–43.

Alberto AV, Faria RX, Couto CG, Ferreira LG, Souza CA, Teixeira PC, et al. Is pannexin the pore associated with the P2X7 receptor? Naunyn Schmiedebergs Arch Pharmacol 2013; 386: 775–87.

Ayata C, Jin H, Kudo C, Dalkara T, Moskowitz MA. Suppression of cortical spreading depression in migraine prophylaxis. Ann Neurol 2006; 59: 652–61.

Ayata C. Pearls and pitfalls in experimental models of spreading depression. Cephalalgia 2013; 33: 604–13.

Balkaya M, Endres M. Behavioral testing in mouse models of stroke. Rodent Models Stroke 2010; 47: 18.

Bohar Z, Nagy-Grocz G, Fejes-Szabo A, Tar L, Laszlo AM, Buki A, et al. Diverse effects of Brilliant Blue G administration in models of trigeminal activation in the rat. J Neural Transm (Vienna) 2015; 122: 1621–31.

Bolay H, Reuter U, Dunn AK, Huang Z, Boas DA, Moskowitz MA. Intrinsic brain activity triggers trigeminal meningeal afferents in a migraine model. Nat Med 2002; 8: 136–42.

Buisman HP, Steinberg TH, Fischbarg J, Silverstein SC, Vogelzang SA, Ince C, et al. Extracellular ATP induces a large nonselective conductance in macrophage plasma membranes. Proc Natl Acad Sci USA 1988; 85: 7988–92.

Cervetto C, Alloisio S, Frattaroli D, Mazzotta MC, Milanese M, Gavazzo P, et al. The P2X7 receptor as a route for non-exocytotic glutamate release: dependence on the carboxyl tail. J Neurochem 2013; 124: 821–31.

Cervetto C, Mazzotta MC, Frattaroli D, Alloisio S, Nobile M, Maura G, et al. Calmidazolium selectively inhibits exocytotic glutamate release evoked by P2X7 receptor activation. Neurochem Int 2012; 60: 768–72.

Chen S, Ma Q, Krafft PR, Hu Q, Rolland W, Sherchan, P, II et al. P2X7R/cryopyrin inflammasome axis inhibition reduces neuroinflammation after SAH. Neurobiol Dis 2013; 58: 296–307.

Chen SP, Ayata C. Spreading depression in primary and secondary headache disorders. Curr Pain Headache Rep 2016; 20: 44.

Chessell IP, Michel AD, Humphrey PP. Effects of antagonists at the human recombinant P2X7 receptor. Br J Pharmacol 1998; 124: 1314–20.

Chu K, Yin B, Wang J, Peng G, Liang H, Xu Z, et al. Inhibition of P2X7 receptor ameliorates transient global cerebral ischemia/reperfusion injury via modulating inflammatory responses in the rat hippocampus. J Neuroinflammation 2012; 9: 69.

Clark AK, Staniland AA, Marchand F, Kaan TK, McMahon SB, Malcangio M. P2X7-dependent release of interleukin-1beta and nociception in the spinal cord following lipopolysaccharide. J Neurosci 2010; 30: 573–82.

Csolle C, Baranyi M, Zsilla G, Kittel A, Goloncser F, Illes P, et al. Neurochemical changes in the mouse hippocampus underlying the antidepressant effect of genetic deletion of P2X7 receptors. PLoS One 2013; 8: e66547.

Di Cesare Mannelli L, Marcoli M, Micheli L, Zanardelli M, Maura G, Ghelardini C, et al. Oxaliplatin evokes P2X7-dependent glutamate release in the cerebral cortex: a pain mechanism mediated by Pannexin 1. Neuropharmacology 2015; 97: 133–41.

Donnelly-Roberts DL, Namovic MT, Han P, Jarvis MF. Mammalian P2X7 receptor pharmacology: comparison of recombinant mouse, rat and human P2X7 receptors. Br J Pharmacol 2009; 157: 1203–14.

Eikermann-Haerter K, Dilekoz E, Kudo C, Savitz SI, Waeber C, Baum MJ, et al. Genetic and hormonal factors modulate spreading depression and transient hemiparesis in mouse models of familial hemiplegic migraine type 1. J Clin Invest 2009; 119: 99–109.

Eikermann-Haerter K, Can A, Ayata C. Pharmacological targeting of spreading depression in migraine. Expert Rev Neurother 2012a; 12: 297–306.

Eikermann-Haerter K, Lee JH, Yuzawa I, Liu CH, Zhou Z, Shin HK, et al. Migraine mutations increase stroke vulnerability by facilitating ischemic depolarizations. Circulation 2012b; 125: 335–45.

Eikermann-Haerter K, Yuzawa I, Dilekoz E, Joutel A, Moskowitz MA, Ayata C. Cerebral autosomal dominant arteriopathy with subcortical infarcts and leukoencephalopathy syndrome mutations increase susceptibility to spreading depression. Ann Neurol 2011; 69: 413–18.

Eising E, Shyti R, 't Hoen PA, Vijfhuizen LS, Huisman SM, Broos LA, et al. Cortical spreading depression causes unique dysregulation of inflammatory pathways in a transgenic mouse model of migraine. Mol Neurobiol 2016, doi:10.1007/s12035-015-9681-5.

Ferrari MD, Klever RR, Terwindt GM, Ayata C, van den Maagdenberg AM. Migraine pathophysiology: lessons from mouse models and human genetics. Lancet Neurol 2015; 14: 65–80.

Goloncser F, Sperlagh B. Effect of genetic deletion and pharmacological antagonism of P2X7 receptors in a mouse animal model of migraine. J Headache Pain 2014; 15: 24.

Gulbransen BD, Bashashati M, Hirota SA, Gui X, Roberts JA, MacDonald JA, et al. Activation of neuronal P2X7 receptor-pannexin-1 mediates death of enteric neurons during colitis. Nat Med 2012; 18: 600–4.

Hadjikhani N, Sanchez Del Rio M, Wu O, Schwartz D, Bakker D, Fischl B, et al. Mechanisms of migraine aura revealed by functional MRI in human visual cortex. Proc Natl Acad Sci USA 2001; 98: 4687–92.

Iglesias R, Locovei S, Roque A, Alberto AP, Dahl G, Spray DC, et al. P2X7 receptor-Pannexin1 complex: pharmacology and signaling. Am J Physiol Cell Physiol 2008; 295: C752–60.

Karatas H, Erdener SE, Gursoy-Ozdemir Y, Lule S, Eren-Kocak E, Sen ZD, et al. Spreading depression triggers headache by activating neuronal Panx1 channels. Science 2013; 339: 1092–5.

Keystone EC, Wang MM, Layton M, Hollis S, McInnes IB. Clinical evaluation of the efficacy of the P2X7 purinergic receptor antagonist AZD9056 on the signs and symptoms of rheumatoid arthritis in patients with active disease despite treatment with methotrexate or sulphasalazine. Ann Rheum Dis 2012; 71: 1630–5.

Lambertsen KL, Biber K, Finsen B. Inflammatory cytokines in experimental and human stroke. J Cereb Blood Flow Metab 2012; 32: 1677–98.

Li L, Fei Z, Ren J, Sun R, Liu Z, Sheng Z, et al. Functional imaging of interleukin 1 beta expression in inflammatory process using bioluminescence imaging in transgenic mice. BMC Immunol 2008; 9: 49.

Li X, Wang X. Application of real-time polymerase chain reaction for the quantitation of interleukin-1beta mRNA upregulation in brain ischemic tolerance. Brain Res Brain Res Protoc 2000; 5: 211–17.

Locovei S, Scemes E, Qiu F, Spray DC, Dahl G. Pannexin1 is part of the pore forming unit of the P2X(7) receptor death complex. FEBS Lett 2007; 581: 483–8.

Moskowitz MA, Nozaki K, Kraig RP. Neocortical spreading depression provokes the expression of c-fos protein-like immunoreactivity within trigeminal nucleus caudalis via trigeminovascular mechanisms. J Neurosci 1993; 13: 1167–77.

Neeb L, Hellen P, Boehnke C, Hoffmann J, Schuh-Hofer S, Dirnagl U, et al. IL-1beta stimulates COX-2 dependent PGE(2) synthesis and CGRP release in rat trigeminal ganglia cells. PLoS One 2011; 6: e17360.

Pan HC, Chou YC, Sun SH. P2X7 R-mediated Ca(2+) -independent d-serine release via pannexin-1 of the P2X7 R-pannexin-1 complex in astrocytes. Glia 2015; 63: 877–93.

Pelegrin P, Surprenant A. Pannexin-1 mediates large pore formation and interleukin-1beta release by the ATP-gated P2X7 receptor. EMBO J 2006; 25: 5071–82.

Pelegrin P, Surprenant A. The P2X(7) receptor-pannexin connection to dye uptake and IL-1beta release. Purinergic Signal 2009; 5: 129–37.

Pietrobon D, Moskowitz MA. Chaos and commotion in the wake of cortical spreading depression and spreading depolarizations. Nat Rev Neurosci 2014; 15: 379–93.

Poornima V, Madhupriya M, Kootar S, Sujatha G, Kumar A, Bera AK. P2X7 receptor-pannexin 1 hemichannel association: effect of extracellular calcium on membrane permeabilization. J Mol Neurosci 2012; 46: 585–94.

Pusic KM, Pusic AD, Kemme J, Kraig RP. Spreading depression requires microglia and is decreased by their M2a polarization from environmental enrichment. Glia 2014; 62: 1176–94.

Rioja I, Bush KA, Buckton JB, Dickson MC, Life PF. Joint cytokine quantification in two rodent arthritis models: kinetics of expression, correlation of mRNA and protein levels and response to prednisolone treatment. Clin Exp Immunol 2004; 137: 65–73.

Salas E, Carrasquero LM, Olivos-Ore LA, Bustillo D, Artalejo AR, Miras-Portugal MT, et al. Purinergic P2X7 receptors mediate cell death in mouse cerebellar astrocytes in culture. J Pharmacol Exp Ther 2013; 347: 802–15.

Somjen GG. Mechanisms of spreading depression and hypoxic spreading depression-like depolarization. Physiol Rev 2001; 81: 1065–96.

Sorge RE, Trang T, Dorfman R, Smith SB, Beggs S, Ritchie J, et al. Genetically determined P2X7 receptor pore formation regulates variability in chronic pain sensitivity. Nat Med 2012; 18: 595–9.

Stock TC, Bloom BJ, Wei N, Ishaq S, Park W, Wang X, et al. Efficacy and safety of CE-224,535, an antagonist of P2X7 receptor, in treatment of patients with rheumatoid arthritis inadequately controlled by methotrexate. J Rheumatol 2012; 39: 720–7.

van den Maagdenberg AM, Pietrobon D, Pizzorusso T, Kaja S, Broos LA, Cesetti T, et al. A Cacna1a knockin migraine mouse model with increased susceptibility to cortical spreading depression. Neuron 2004; 41: 701–10.

van den Maagdenberg AM, Pizzorusso T, Kaja S, Terpolilli N, Shapovalova M, Hoebeek FE, et al. High cortical spreading

depression susceptibility and migraine-associated symptoms in Ca(v)2.1 S218L mice. Ann Neurol 2010; 67: 85–98.
Virginio C, Church D, North RA, Surprenant A. Effects of divalent cations, protons and calmidazolium at the rat P2X7 receptor. Neuropharmacology 1997; 36: 1285–94.
Walsh JG, Muruve DA, Power C. Inflammasomes in the CNS. Nat Rev Neurosci 2014; 15: 84–97.
Wang J, Jackson DG, Dahl G. The food dye FD&C Blue No. 1 is a selective inhibitor of the ATP release channel Panx1. J Gen Physiol 2013; 141: 649–56.
Weilinger NL, Tang PL, Thompson RJ. Anoxia-induced NMDA receptor activation opens pannexin channels via Src family kinases. J Neurosci 2012; 32: 12579–88.
Yamasaki Y, Matsuura N, Shozuhara H, Onodera H, Itoyama Y, Kogure K. Interleukin-1 as a pathogenetic mediator of ischemic brain damage in rats. Stroke 1995; 26: 676–80; discussion 81.
Yegutkin GG, Guerrero-Toro C, Kilinc E, Koroleva K, Ishchenko Y, Abushik P, et al. Nucleotide homeostasis and purinergic nociceptive signaling in rat meninges in migraine-like conditions. Purinergic Signal 2016; 12: 561–74.
Zhang X, Burstein R, Levy D. Local action of the proinflammatory cytokines IL-1beta and IL-6 on intracranial meningeal nociceptors. Cephalalgia 2012; 32: 66–72.
Zhang Y, Saccani S, Shin H, Nikolajczyk BS. Dynamic protein associations define two phases of IL-1beta transcriptional activation. J Immunol 2008; 181: 503–12.